

Article

# Coaxial Helicopter Attitude Control System Design by Advanced Model Predictive Control under Disturbance

Zhi Chen <sup>1</sup>, Xiangyu Lin <sup>1</sup> and Wanyue Jiang <sup>2,\*</sup>

<sup>1</sup> School of Mechatronic Engineering and Automation, Shanghai University, Shanghai 200444, China; andychen183@shu.edu.cn (Z.C.); 13950689387@163.com (X.L.)

<sup>2</sup> School of Automation, Qingdao University, Qingdao 266071, China

\* Correspondence: jwy@qdu.edu.cn

**Abstract:** This paper proposes an advanced model predictive control (MPC) scheme for the attitude tracking of coaxial drones under wind disturbances. Unlike most existing MPC setups, this scheme embeds steady-input, steady-output, and steady-state conditions into the optimization problem as decision variables. Consequently, the coaxial drone's attitude can slide along the state manifold composed of a series of steady states. This allows it to move toward the optimal reachable equilibrium. To address disturbances that are difficult to accurately measure, an extended state observer is employed to estimate the disturbances in the prediction model. This design ensures that the algorithm maintains recursive stability even in the presence of disturbances. Finally, numerical simulations and flight tests are provided to confirm the effectiveness of the proposed method through comparison with other control algorithms.

**Keywords:** attitude control; model predictive control; disturbance observer

## 1. Introduction

Unmanned aerial vehicles (UAVs) have been developed at an astonishing pace over the past 30 years. Common UAV types include fixed-wing and rotary-wing designs. Among these, the coaxial dual-rotor UAV possesses unique advantages such as compact structure, strong stability, high payload capacity, and high forward speed. Leveraging these benefits, coaxial UAVs have the potential to replace humans in performing numerous hazardous tasks.

Currently, the use of unmanned aerial vehicles (UAVs) is steadily increasing across various fields. Correspondingly, there has been a growing investment in UAV research, with particular emphasis on control methods. Multirotor UAVs constitute underactuated nonlinear systems with coupled states. They have six degrees of freedom (position:  $x$ ,  $y$ ,  $z$ ; orientation: roll, pitch, yaw), yet their control inputs are typically less than six. Additionally, despite the existence of generic models for UAVs, when considering specific flight conditions, numerous complex factors need to be taken into account, such as parameter uncertainties, external disturbances, and unmodeled dynamics [1]. In recent years, various control methods have been employed to address the dynamic characteristics of UAVs [2–5].

In [6], robust PID controllers are applied to quadcopter UAVs for trajectory tracking tasks and minimizing power consumption. Noormohammadi-Asl et al. [7] obtained both the nominal linear model of the system and the uncertainty model containing the deviation between the nonlinear system and the nominal model by identifying the system through frequency response in the case of parameter uncertainty in the system. Then, a linear H controller was designed to control the attitude of the UAV, which successfully achieved the goals of attitude tracking, interference suppression, and input saturation. Hossam, A. et al. [8] proposed a Mu-based quadrotor trajectory tracking control method that can suppress different types of disturbances and is able to deal with uncertainties of even infinite dimensions, such as time delay, effectively. The proposed approach covers a weakly



**Citation:** Chen, Z.; Lin, X.; Jiang, W. Coaxial Helicopter Attitude Control System Design by Advanced Model Predictive Control under Disturbance. *Aerospace* **2024**, *11*, 486. <https://doi.org/10.3390/aerospace11060486>

Academic Editor: Gokhan Inalhan

Received: 31 March 2024

Revised: 10 June 2024

Accepted: 12 June 2024

Published: 19 June 2024



**Copyright:** © 2024 by the authors. Licensee MDPI, Basel, Switzerland. This article is an open access article distributed under the terms and conditions of the Creative Commons Attribution (CC BY) license (<https://creativecommons.org/licenses/by/4.0/>).

nonlinear range of operation, which is reasonable for many applications, while maintaining low computational cost, since the controller is linear and fixed. The controller was tested via a realistic simulation environment and compared to an LQR controller. According to the simulations, the proposed controller has superior performance, even in the presence of time delays and disturbances.

In [9,10], the authors propose a new method for terminal sliding mode control to achieve time-synchronous convergence of multiple-input-multiple-output (MIMO) systems under disturbances. In [11], the flight tracking control problem in the UAV altitude and attitude control system under full state constraints is studied by the output feedback control scheme. Under the designed flight output feedback tracking controller, the unmanned helicopter altitude and attitude control system achieves the expected control objectives within the state limits. In [12], an INDI-based actuator compensation attitude controller is developed for the helicopter subject to the time delay, position, and rate saturations in actuators. The controller is composed of a rate controller which ensures the rate performance of the helicopter, an attitude controller which guarantees the attitude tracking performance, and a collective pitch controller which meets the needs of the vertical changes in the z-axis direction. The model reduction method is used to design an INDI-based controller for the rate loop and collective pitch of the main rotor, which improves the robustness to the time-varying actuator delay.

Traditional control methods have made outstanding achievements in UAV control. However, there are various constraints in the actual flight system. Therefore, a model predictive control algorithm that can solve the optimization problem with various constraints online has attracted the attention of researchers.

Researchers have adopted a large number of model predictive control methods on UAVs [13–18], combining neural networks and reinforcement learning with model predictive control [19–23]. In these works, the nonlinear MPC algorithm proposed by the authors reduces computational complexity while ensuring trajectory tracking accuracy [13], and the authors [17] transform the nonlinear model into a controllable linear system in Brunovsky Canonical Form through the differential flatness theory. In view of the influence of complex aerodynamic effects generated by UAVs under high-speed motion, an MPC controller incorporated into the Gaussian process was designed to accurately and efficiently control the aerodynamic effects of the model in real time, which greatly reduced the trajectory tracking error [20]. In [22], a real-time neural network MPC is proposed, which integrates a large complex neural network architecture as a framework for dynamic models in the model predictive control pipeline. Experiments were carried out on a highly agile quadcopter platform to demonstrate the operational capabilities of the described system.

Previous research has achieved significant success in trajectory tracking. However, most of these works primarily focused on the dynamics model of the aircraft itself, neglecting potential external disturbance effects. When drones face scenarios with disturbances, the more complex dynamic effects, if ignored by the controller, can easily lead to tracking deviations or even loss of control. Addressing the disturbance problem is a crucial step for drones to transition from indoor experimental environments to real-world outdoor flight scenarios.

In this paper, we propose a disturbance-affected unmanned aerial vehicle (UAV) attitude tracking controller based on model predictive control (MPC). Inspired by [24,25], the proposed controller achieves precise control of nonlinear systems by utilizing a linear time-varying (LTV) model. The main contributions are as follows:

Firstly, the controller takes into account external disturbances present during actual drone flight and the linearization errors resulting from the use of linearized models. Treating these disturbances as a lumped disturbance, we design a linear extended state observer to accurately estimate the disturbances in the predictive model. In the case of disturbances being continuously bounded, this observer is able to converge within a finite time and ensures the continuity of the observer's output.

Secondly, compared to traditional LTV-MPC, this controller uses the system's steady-state equilibrium point as a decision variable in the cost function, reducing the requirement for an accurate linearization model and improving the stability of the control algorithm.

The remaining structure of this paper is as follows. In Section 2, we describe the coaxial UAV attitude dynamics model in detail. In Section 3, we describe the implementation details of the UAV attitude controller, including the design of the linear extended state observer and the implementation of advanced MPC. Then, experiment is given to verify the proposed control scheme in Section 4. And finally, the conclusion is given in Section 5.

## 2. System Model

In this paper, we study a coaxial drone shown in Figure 1a. Its flight relies on the upper and lower rotors to provide lift, and the attitude angle of the drone is controlled by changing the angle between the rotor and the main axis of the aircraft.

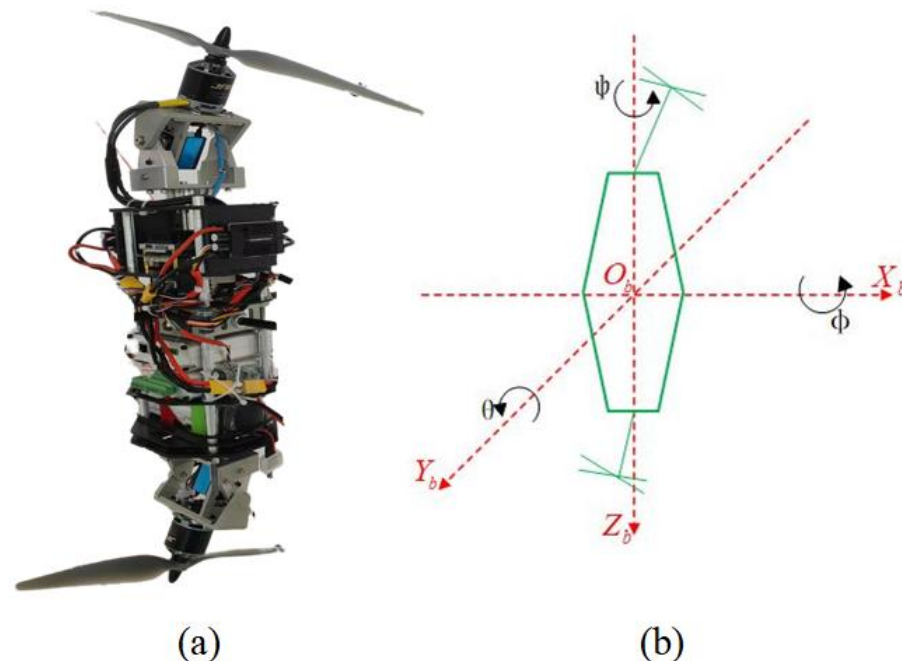


**Figure 1.** (a) Coaxial drone; (b) diagram of coordinate systems on coaxial drone.

The coordinate system and physical quantities of the coaxial drone studied in this paper are shown in Figure 1b. In the figure, the airframe and airborne coordinate system are used as the NED coordinate system.  $(\varphi, \theta, \psi)$  signifies a set of Euler angles used to describe the helicopter's attitude relative to the NED frame. The drone is regarded as a rigid structure, and the gyroscopic effect caused by the rotation of the motor is ignored. The attitude model of the UAV using the Newton–Euler method is as follows [11]:

$$\begin{aligned}\dot{\Omega} &= W_b(\Omega)\omega_b \\ \dot{\omega}_b &= J^{-1}[M_b - \omega_b \times (J\omega_b)]\end{aligned}\quad (1)$$

where  $\dot{\Omega} = (\dot{\varphi} \ \dot{\theta} \ \dot{\psi})^T$ , and  $\varphi, \theta, \psi$  denote the roll angle, pitch angle, and yaw angle of the UAV, respectively.  $W_b(\Omega)$  is the angular velocity transformation matrix, which is shown as follows:

$$W_b(\Omega) = \begin{bmatrix} 1 & \tan \theta \sin \phi & \tan \theta \cos \phi \\ 0 & \cos \phi & -\sin \phi \\ 0 & \frac{\sin \phi}{\cos \theta} & \frac{\cos \phi}{\cos \theta} \end{bmatrix}$$

In addition,  $\omega_b(t) = ( p(t) \ q(t) \ r(t) )^T$ , and  $p(t)$ ,  $q(t)$ , and  $r(t)$  denote the roll, pitch, and yaw angular velocities, respectively;  $J$  denotes the moment of inertia of the body. Since the inertia tensor of the non-spindle is extremely small, the non-spindle quantity can be ignored, so  $J = \text{diag}\{ I_x \ I_y \ I_z \}$ ;  $M_b = ( U_x \ U_y \ U_z )^T$  denotes the control input torque of the coaxial drone, and “ $\times$ ” is the multiplication cross matrix.

Equation (2) is obtained by expanding the vectors and matrices in Equation (1):

$$\left\{ \begin{array}{l} \begin{bmatrix} \dot{\phi} \\ \dot{\theta} \\ \dot{\varphi} \end{bmatrix} = \begin{bmatrix} 1 & \tan \theta \sin \phi & \tan \theta \cos \phi \\ 0 & \cos \phi & -\sin \phi \\ 0 & \frac{\sin \phi}{\cos \theta} & \frac{\cos \phi}{\cos \theta} \end{bmatrix} \begin{bmatrix} p(t) \\ q(t) \\ r(t) \end{bmatrix} \\ \begin{bmatrix} \dot{p}(t) \\ \dot{q}(t) \\ \dot{r}(t) \end{bmatrix} = \begin{bmatrix} \frac{1}{I_x} & 0 & 0 \\ 0 & \frac{1}{I_y} & 0 \\ 0 & 0 & \frac{1}{I_z} \end{bmatrix} \left[ \begin{bmatrix} U_x \\ U_y \\ U_z \end{bmatrix} - \begin{bmatrix} p \\ q \\ r \end{bmatrix} \times \left( \begin{bmatrix} I_x & 0 & 0 \\ 0 & I_y & 0 \\ 0 & 0 & I_z \end{bmatrix} \begin{bmatrix} p \\ q \\ r \end{bmatrix} \right) \right] \end{array} \right. \quad (2)$$

We select  $x = [\phi, \theta, \psi, p, q, r]^T$  as the state vector of the system,  $u = [U_x, U_y, U_z]^T$  as the control input of the system, and  $y = [\phi, \theta, \varphi]^T$  as the output of the system. The complete nonlinear model can be obtained by replacing the left side of Equation (2) with  $x$  and expanding the right side as follows:

$$\dot{x} = \begin{bmatrix} p + \tan \theta \cos \phi \cdot r + \tan \theta \sin \phi \cdot q \\ \cos \phi \cdot q - \sin \phi \cdot r \\ \frac{\sin \phi}{\cos \theta} \cdot q + \frac{\cos \phi}{\cos \theta} \cdot r \\ \frac{I_y - I_z}{I_x} qr + \frac{U_x}{I_x} \\ \frac{I_z - I_x}{I_y} pr + \frac{U_y}{I_y} \\ \frac{I_x - I_y}{I_z} pq + \frac{U_z}{I_z} \end{bmatrix} = f(x_t, u_t) \quad (3)$$

This nonlinear model  $f(x_t, u_t)$  is an affine form of the state of the system. Since the MPC algorithm prediction model adopted in this paper needs to adopt the linearization model of the current point, the Jacobian linearization method is used to convert the nonlinear model of the UAV into the linear time-varying (LTV) state space equation as follows:

$$\begin{cases} \dot{x}(t) = A(t_0)x(t) + B(t_0)u(t) + E(t_0) \\ y(t) = Cx(t) \end{cases} \quad (4)$$

where  $A(t_0) := \frac{\partial f}{\partial x} \Big|_{x_0, u_0}$ ,  $B(t_0) := \frac{\partial f}{\partial u} \Big|_{x_0, u_0}$  is obtained by finding the partial derivatives of the state and the input by the nonlinear equation at  $t_0$ ;  $E(t_0)$  denotes the model error caused by the linearization of nonlinear equations;  $C = [ I_3 \ O ]$ , where  $I_3$  is a 3rd-order identity matrix and  $O$  is a 3rd-order zero matrix.

### 3. Attitude Control System Design

During UAV missions, the flight environment is often complex and unpredictable disturbances exist. Neglecting these disturbances can have a significant impact on UAV control, potentially leading to catastrophic consequences such as UAV crashes. In order to prevent the occurrence of catastrophic events, this paper uses the method of a linear state control observer to estimate the overall disturbance and design an MPC controller based on the equilibrium setpoint to achieve accurate control of the UAV attitude. The block diagram of the attitude control system consisting of ESO and MPC is shown in Figure 2.

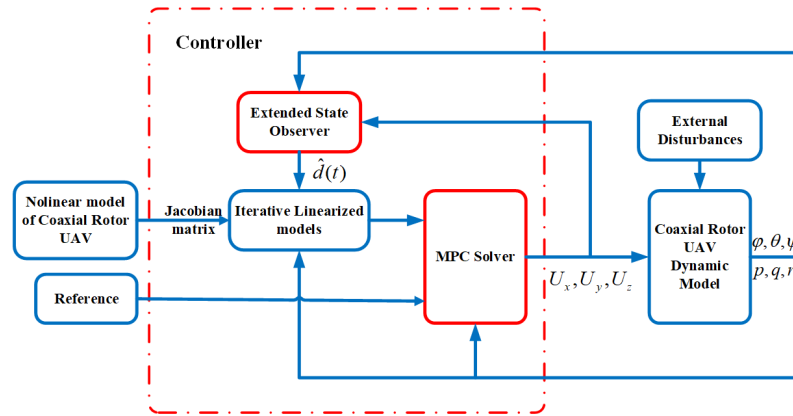


**Figure 2.** A schematic of the proposed attitude control system.

### 3.1. Extended State Observer for Disturbance Estimation

During flight, disturbances cannot be measured directly by sensors. A state observer can estimate the state variables of a system using the actual inputs and outputs of the system. The extended state observer (ESO) is the core of the Active Disturbance Rejection Controller (ADRC), which adds the disturbance of the system to the state vector of the system to obtain an extended state vector containing the disturbance, and then the state of the system and the disturbance of the system can be calculated by using the properties of the state observer.

Consider the existence of a linear bounded external perturbation for the attitude angular velocity channel. Merge the external disturbances with  $E(t_0)$  into a lumped disturbance  $d(t) = [e_x \ e_y \ e_z]^T$  as the expanded state quantity, and then define a new state vector  $x_{obs} = [x \ d(t)]^T$ . And let the derivative of  $d(t)$  be  $h$ ; then, the expanded state space equation is:

$$\begin{cases} \dot{x}_{obs} = A_{obs}x_{obs}(t) + B_{obs}u(t) + Eh \\ y = C_{obs}x_{obs}(t) \end{cases} \quad (5)$$

where:

$$A_{obs} = \begin{bmatrix} A(t_0)_{6 \times 6} & 0_{3 \times 3} \\ 0_{3 \times 6} & I_{3 \times 3} \end{bmatrix}, B_{obs} = \begin{bmatrix} B(t_0) \\ 0_{3 \times 3} \end{bmatrix}, E = \begin{bmatrix} 0_{6 \times 6} \\ I_{3 \times 3} \end{bmatrix}, C_{obs} = [C \ 0_{3 \times 3}]$$

Based on system (5), a Luenberger linear state observer is designed. The state vector of the observer is  $\hat{x}_{obs}$ . The estimated expressions for the state and output of the observer are as follows:

$$\begin{cases} \dot{\hat{x}}_{obs} = A_{obs}\hat{x}_{obs} + B_{obs}u + L(y - \hat{y}) \\ \hat{y} = C_{obs}\hat{x} \end{cases} \quad (6)$$

Equation (5) is subtracted from Equation (6) to obtain:

$$\dot{e} = (A_{obs} - LC_{obs})e - Eh \quad (7)$$

where  $e = x_{obs} - \hat{x}_{obs}$ .

By making all the eigenroots of  $(A_{obs} - LC_{obs})$  fall to the left half of the complex plane through the pole configuration, the error  $e$  will converge to 0 with time, that is, the designed observer can quickly estimate all the state quantities of the system. After the feedback gain

matrix  $L$  is inversely solved by the configured poles, the extended state space expression can be written as:

$$\begin{cases} \hat{x}_{obs} = (A_{obs} - LC_{obs})\hat{x}_{obs} + [B_{obs}; L] \begin{bmatrix} u \\ y \end{bmatrix} \\ \hat{y} = I_9\hat{x}_{obs} \end{cases} \quad (8)$$

where  $\hat{x}_{obs} = [ \hat{x} \quad \hat{d}(t) ]^T$ ,  $\hat{d}(t)$  denotes the perturbation value estimated by the observer, and  $M$  is the ninth-order identity matrix.

**Remark 1.** In this paper, the disturbance estimation method is used as a linear extended state observer. Although the UAV flight environment is complex and the disturbances are frequent and difficult to estimate, in the case of low-speed flight, most of the disturbances that can affect UAV flight are mostly wind disturbances. We can consider that  $d(t)$  is bounded, i.e., there exists a known real number  $\mathbf{D} \in \mathbb{R}_+$ , such that  $|d(t)| \leq \mathbf{D}$ . Therefore, we believe that the observer we designed has the conditions for convergence in such a perturbation environment.

### 3.2. Advanced MPC Framework

Model predictive control is a form of control in which the current control action is obtained by solving, at each sampling instant, a finite horizon open-loop optimal control problem, using the current state of the plant as the initial state; the optimization yields an optimal control sequence and the first control in this sequence is applied to the plant [26]. For the LTV model of a coaxial UAV with disturbance, an MPC based on a steady-state setpoint is designed in this paper. In order to meet the needs of the optimization problem in the fast-solving algorithm, the zero-order holding method is used to rewrite the continuous time–state space equation of the above model (5) into a discrete time–state space equation:

$$\begin{cases} x(k+1) = A_kx(k) + B_ku(k) + B_d d(k) \\ y(k) = C_kx(k) \end{cases} \quad (9)$$

The solution of the optimal problem of the proposed algorithm produces the best nominal state and input, steady-state input, output, and state, and the proposed cost function is as follows, which is a combination of the error between the nominal state and the steady-state input, the input and the steady-state input, and the steady-state output and the reference:

$$J = \min_{\substack{\bar{x}(t), \bar{u}(t) \\ x^s(t), u^s(t) \\ y^s(t)}} \sum_{k=0}^{N-1} \|x_k(t) - x^s(t)\|_Q^2 + \|u_k(t) - u^s(t)\|_R^2 + \|y^s(t) - y^r\|_S^2 \quad (10a)$$

$$\text{s.t. } x_{k+1}(t) = A_{x_t}x_k(t) + Bu_k(t) + B_d d(k) \quad (10b)$$

$$x_0(t) = x_t, \quad x_N(t) = x^s(t) \quad (10c)$$

$$(x^s(t), u^s(t)) \in \mathcal{Z}_{Lin}^s(x_t) \quad (10d)$$

$$y^s(t) = C_{x_t}x^s(t) + Du^s(t). \quad (10e)$$

where  $x_k(t)$  represents the value of the state predicted by the system at the  $k$ th step at time  $t$ ;  $u_k(t)$  denotes the value of the control input predicted by the system at time  $t$  at the  $k$ th step.  $(x^s(t), u^s(t), y^s(t))$  is the sequence of equilibrium points selected at time  $t$ ;  $N$  denotes the predicted step size;  $Q, R, S$  are positively definite weight matrices.  $\mathcal{Z}_{Lin}^s(x_t)$  is a steady-state set of systems.

Compared with the common MPC algorithm, this algorithm solves the optimal problem based on the linearization model of each current moment and adds  $(x^s(t), u^s(t), y^s(t))$  as the optimal value to the cost function of the optimal problem. Since  $(x^s(t), u^s(t), y^s(t))$  are uniquely determined by constraint (10e), we can select an artificially set steady-state

point  $(x^s(t), u^s(t), y^s(t))$  near the reference value  $y^r$  to meet the equilibrium condition and optimize the distance from the steady-state point to the reference trajectory online. At the same time, the goal of system optimization is also changed from the distance to the reference trajectory to the distance to the equilibrium point. In addition, due to the existence of constraint (10c), the system can reach the equilibrium point after  $N$  prediction steps, which has the same effect as the terminal penalty in the traditional MPC, and it can also be changed to add an item to the optimized cost function  $\|x_N(t) - x^s(t)\|_p^2$ .

Since the weight matrices  $Q, R,$  and  $S$  are all positively definite, Problem (10) becomes a convex QP [27]. Based on the properties of convex QP, we know that the objective function has a unique optimal solution  $(x_k(t), u_k(t), x^s(t), u^s(t), y^s(t))$ . Problem (10) is a convex quadratic problem, so the algorithm can always find the optimal value quickly, while solving the nonlinear MPC of the non-convex problem is relatively difficult and time-consuming. In addition, although they all rely on linearized iterative prediction models at setpoints, traditional LTV-MPC has additional boundary requirements for linearization errors. The artificial steady-state setpoint algorithm satisfies the stability condition that the initial state of the system is close to the steady-state manifold, even if the initial state of the system is far away from the setpoint; as long as the initial state is close to the steady-state manifold, the algorithm can still remain stable. When the initial state is far from the setpoint, the stability of LTVMPC may not be satisfied. In order for the LTVMPC controller to remain stable and ensure that the linearization error is within the allowable boundary, the sampling time needs to be reduced.

The following proves that the algorithm has recursive stability, and the Lyapunov function candidate is selected as:

$$V(x_t) = J_N^*(x_t) - J_{Lin}^*(x_t) \tag{11}$$

where  $J_N^*(x_t)$  is the case where the optimal value of the cost function  $J$  of the algorithm is obtained;  $J_{Lin}^*(x_t)$  denotes a solution to obtain the optimal value for  $\|y^s(t) - y^r\|_S^2$ .

The system represented by Equation (5) is second-order differentiable. The matrix  $A_{x_t}, B_{x_t}, C_{x_t}$  corresponding to the state space equation satisfies the control ability condition. And for a steady-state output  $y^s(t)$ , there is a unique steady-state  $(x^s(t), u^s(t))$  corresponding to  $y^s(t)$ ;  $x^s(t) = x_{Lin}^{sr}(x_t)$  when  $J_{Lin}^*(x_t)$  obtains the optimal value.

$$\begin{aligned} V(x_t) &= \sum_{k=0}^{N-1} \|x_k(t) - x^s(t)\|_Q^2 + \|u_k(t) - u^s(t)\|_R^2 + \|y^s(t) - y^r\|_S^2 - J_{Lin}^*(x_t) \\ &\leq \sum_{k=0}^{N-1} \|\bar{x}_k(t) - x^s(t)\|_Q^2 + \|\bar{u}_k(t) - u^s(t)\|_R^2 \\ &\leq \lambda_{\max}(Q, R) \sum_{k=0}^{N-1} \left( \|\bar{x}_k(t) - x^s(t)\|_2^2 + \|\bar{u}_k(t) - u^s(t)\|_2^2 \right) \end{aligned} \tag{12}$$

Since the system is controllable, according to the standard theorem of linear system theory, there is a constant  $\Gamma > 0$  for all  $\bar{x} \in \mathbb{R}^n, (x^s, u^s) \in \mathcal{Z}_{Lin}^s(\bar{x})$ , and all initial-state  $x_0$  to  $x_s$ , and it satisfies:

$$\sum_{k=0}^{n-1} \|\hat{x}_k - x^s\|_2 + \|\hat{u}_k - u^s\|_2 \leq \Gamma \|x^s - x_0\|_2. \tag{13}$$

So,

$$\begin{aligned} V(x_t) &\leq \lambda_{\max}(Q, R) \Gamma^2 \|x_t - x_{Lin}^{sr}(x_t)\|_2^2 \\ &= b \|x_t - x_{Lin}^{sr}(x_t)\|_2^2 \end{aligned} \tag{14}$$

**Theorem 1.** *There exist  $V_{\max}, J_{Lin}^{\max} > 0$  such that if  $V \leq V_{\max} J_{Lin}^*(x_t) \leq J_{Lin}^{\max}, J_{Lin}^*(x_{t+n}) \leq J_{Lin}^{\max}$ , there exists a constant  $0 \leq c_V \leq 1$  such that (for more information on the proof process, please refer to [24])*

$$V(x_{t+n}) \leq c_V V(x_t). \tag{15}$$

According to (14), we have:

$$\begin{aligned} V(x_t) &\leq b_1 \|x_t - x_{Lin}^{sr}(x_t)\|_2^2 \\ V(x_{t+n}) &\leq b_2 \|x_{t+n} - x_{Lin}^{sr}(x_{t+n})\|_2^2 \end{aligned} \tag{16}$$

According to (15) and (16), we can obtain that for any moment t there is always:

$$\|x_{t+n} - x_{Lin}^{sr}(x_{t+n})\|_2^2 \leq \frac{b_1}{b_2} c_V \|x_t - x_{Lin}^{sr}(x_t)\|_2^2 \tag{17}$$

Equation (17) shows that the state of the system from time t can converge towards the optimal achievable steady  $x^{sr}(x_t)$  range exponent after n steps, and the output  $y_t$  also converges towards the optimal achievable output  $y^{sr}(x_t)$  exponential. Therefore, the designed MPC algorithm is exponentially stable in a closed loop.

### 4. Simulation Results

#### 4.1. Numerical Simulation

In this section, in order to verify the effectiveness of the proposed controller, the attitude control system of the coaxial dual-rotor UAV is simulated in the MATLAB/Simulink environment. The coaxial drone model parameters are shown in Table 1:

**Table 1.** Coaxial drone parameters.

Variable Name	Variable Symbol	Variable Symbol
Inertia matrix	J	diag{0.0768, 0.0775, 0.0361}
Drone quality	m	2.84 kg
Gravitational acceleration	g	9.8 m/s <sup>2</sup>

For the extended state observer, its pole is configured at  $V = (-40, -32 + 20i, -32 - 20i, -24 + 18i, -24 - 18i, -16 + 12i, -16 - 12i, -5 + 6i, -5 - 6i)$ . For the controller, the forecasting horizon is  $N = 4$  and the weight matrix is  $Q = \text{diag}(100 \ 100 \ 100 \ 10 \ 10 \ 10)$ ,  $R = \text{diag}(0.2 \ 0.2 \ 0.02)$ ,  $S = \text{diag}(1000 \ 1000 \ 1000)$ .

The external disturbance is:

$$d(t) = [ 4 \sin(t) \ 4 \ 4 ]^T$$

The expected attitude angle of the drone is:

$$y_d = [ 0.5 \ 0.2 \ 0.4 ]^T$$

Based on the above parameters, the UAV attitude control system was simulated in the MATLAB/Simulink environment. For comparison, we also applied some controller schemes, each with the same design parameters as above:

- (1) The proposed MPC is the controller using the scheme proposed in Section 3.2 and adopting the expanded state observer proposed in Section 3.1 to estimate the disturbance  $d(k)$  for the prediction Equations (10b) (green line in figure);
- (2) The model-based MPC uses the scheme proposed in [24,25]. The scheme does not consider the disturbances in its predictive models (purple line in figure);
- (3) The ESO-LTV-MPC is an MPC scheme using an LTV prediction model obtained by linearizing the nonlinear dynamics at time t along the candidate solution and adopting the expanded state observer proposed in Section 3.1 to estimate the disturbance  $d(k)$  (red line in figure);
- (4) The SMC is the sliding mode control (yellow line in figure).

Figures 3–5, respectively, show the variation curves of the UAV’s roll, pitch, and yaw angles. Figure 3a presents the tracking curve of the roll angle, while Figure 3b illustrates the error tracking curve. The Proposed MPC controller demonstrates an adjustment time

of approximately 1 s with negligible overshoot and steady-state error. In comparison, the ESO-LTV MPC controller exhibits similar overshoot to the Proposed MPC controller but requires an adjustment time of around 1.2 s. However, it struggles to suppress disturbances effectively, resulting in a steady-state sinusoidal curve with an amplitude of 0.05.

The SMC controller achieves better steady-state error performance than the Proposed MPC controller but suffers from higher overshoot and a longer regulation time. The Model-Based MPC controller, used as a benchmark, lacks an extended state observer to assist in estimating disturbances, causing its prediction model to deviate significantly from the actual model. This deviation leads to a steady-state oscillation error with an amplitude of 0.1 rad in the system.

Figure 3c displays the roll angular velocity, and Figure 3d shows the controller input. Over time, the angular velocity for each controller converges to zero. However, the initial response inputs for the SMC and Model-Based MPC are more abrupt, reaching nearly 8 N·m. During the adjustment period, the SMC input exhibits jitter, while the inputs of the other three algorithms remain smoother.

In summary, from the perspective of roll angle tracking performance, the ESO-Proposed MPC achieves the best results, followed by the SMC, with the ESO-LTV MPC performing the worst.

Figures 4 and 5 show the tracking curves, error tracking curves, and angular velocity changes for the pitch angle and yaw angle, respectively. The conclusions are similar to those for the roll angle. One notable difference is that the Model-Based MPC controller in Figure 4a exhibits a steady-state error of 0.05 rad due to persistent disturbances. In Figure 5a, the Model-Based MPC controller has a steady-state error of 0.1 rad, while the SMC controller shows a steady-state error of more than 0.8 rad. Despite this, the steady-state error remains relatively small.

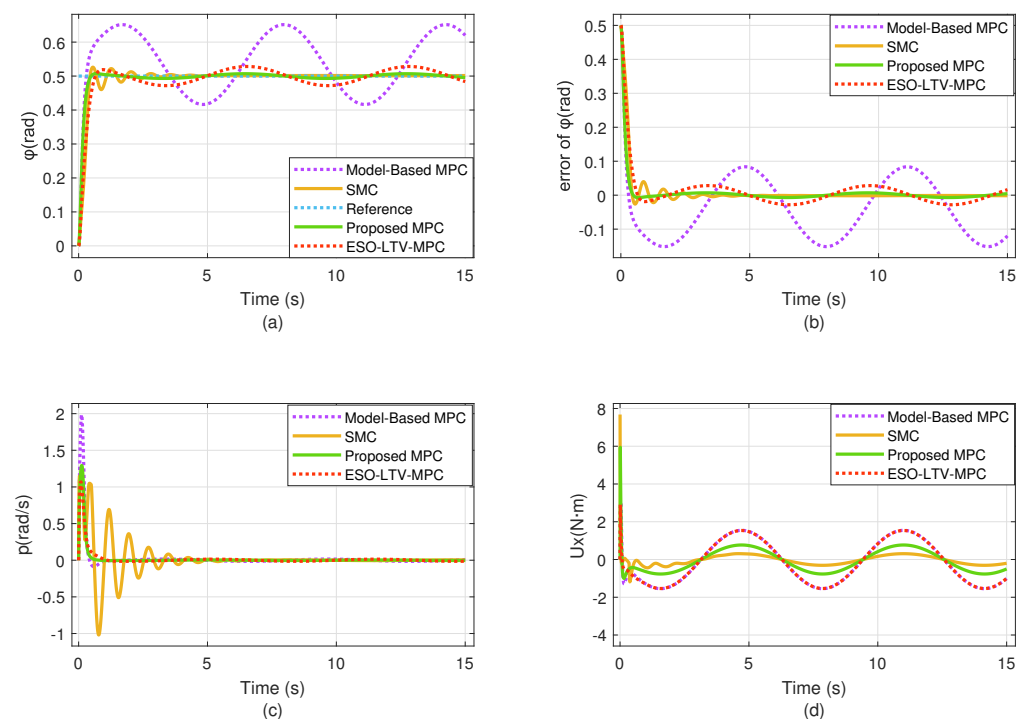


**Figure 3.** The roll channel variable under different controllers: (a) the roll angle; (b) the tracking error of the roll; (c) the attitude velocity of the roll channel; (d) the input of the roll channel.

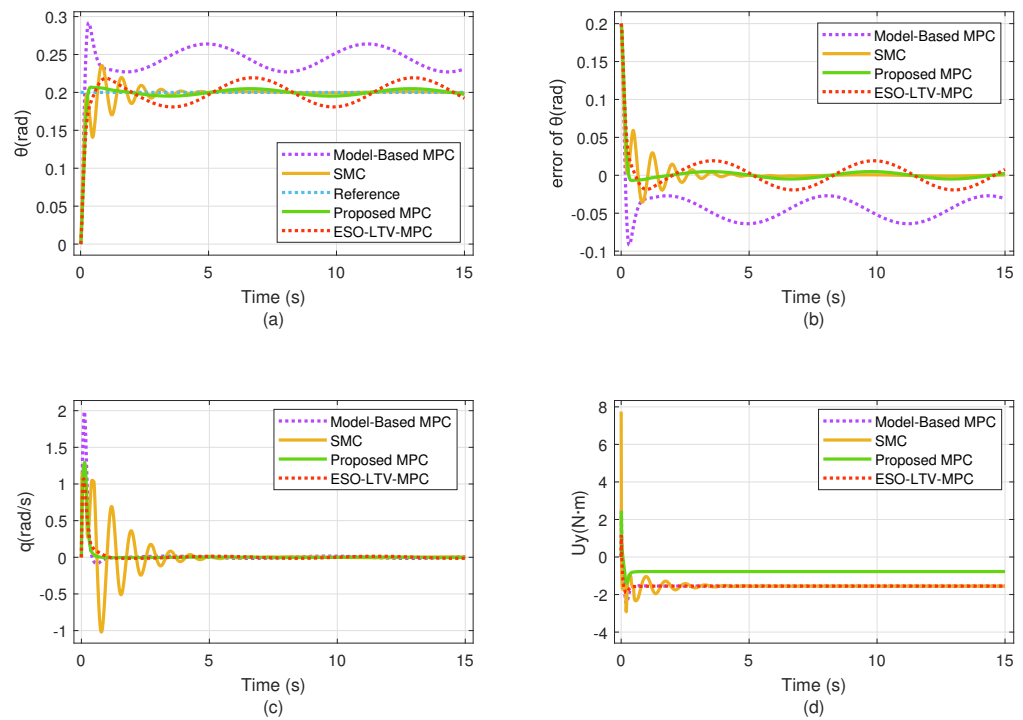


**Figure 4.** The pitch channel variable under different controllers: (a) the pitch angle; (b) the tracking error of the pitch; (c) the attitude velocity of the pitch channel; (d) the input of the pitch channel.

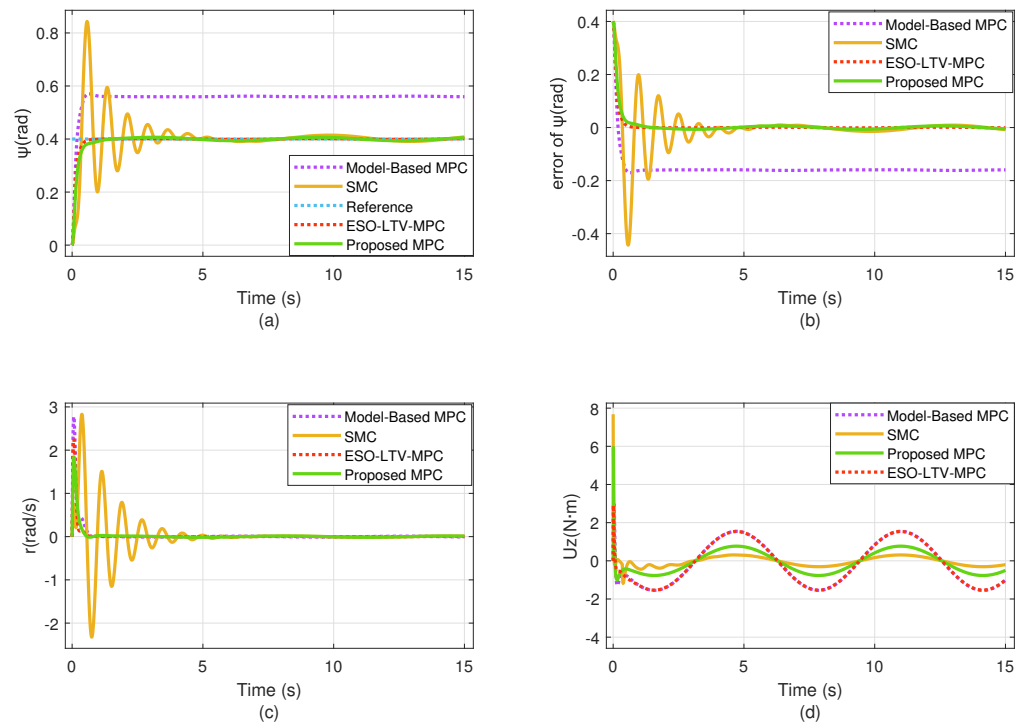


**Figure 5.** The yaw channel variable under different controllers: (a) the yaw angle; (b) the tracking error of the yaw; (c) the attitude velocity of the yaw channel; (d) the input of the yaw channel.

In general, the extended state observer provides an estimate of the external error, enabling the proposed algorithm to resist external disturbances and achieve optimal performance. The Proposed MPC exhibits the shortest regulation time, minimal overshoot, and a negligible steady-state error. While achieving superior tracking of angle changes, the input

of the Proposed MPC is smoother than that of the SMC. Among these control algorithms, the Proposed MPC demonstrates the best overall control performance.

Robustness and recursive stability are also essential considerations for the algorithm. This paper will use a simple simulation experiment to illustrate another advantage of the Proposed MPC controller over the LTV MPC.

Using the same UAV parameters and controller design parameters, both the Proposed MPC controller and the ESO-LTV MPC controller are tasked with tracking the desired attitude angle in the absence of external disturbances and model parameter uncertainty, with a system sampling frequency of 0.05 s:

$$y_d = [ 0.5 \quad 0.2 \quad 0.4 ]^T$$

The initial state of the UAV is:

$$x_0 = [ -0.15 \quad -0.05 \quad 0 \quad 0 \quad 0 \quad 0 ]^T$$

The simulation results are shown in Figures 6–8. Figure 6 illustrates the attitude angle tracking curve of the UAV after a change in the initial state. The data indicate that the system can still stably track the reference attitude angle under the control of the Proposed MPC controller, whereas the system attitude angle diverges under the control of the LTV MPC controller. Figures 7 and 8 show the velocity and input curves. Under the Proposed MPC controller, the velocity and input gradually converge to zero, while under the LTV MPC controller, the curves oscillate between the upper and lower limits.

This instability with the LTV MPC controller is due to an increased output change in the initial state, causing the frequency of the system's linearization updates to lag behind the changes in the control output. As a result, the linearization error exceeds the allowable bounds of the LTV MPC control algorithm, leading to instability. To re-stabilize the algorithm, it would be necessary to shorten the sampling time for system linearization (i.e., increase the sampling frequency) or modify the algorithm's terminal constraints.

In contrast, with the Proposed MPC controller, although the initial state is farther from the reference setpoint, it remains within the vicinity of the controlled system's steady-state manifold, thereby maintaining recursive stability.

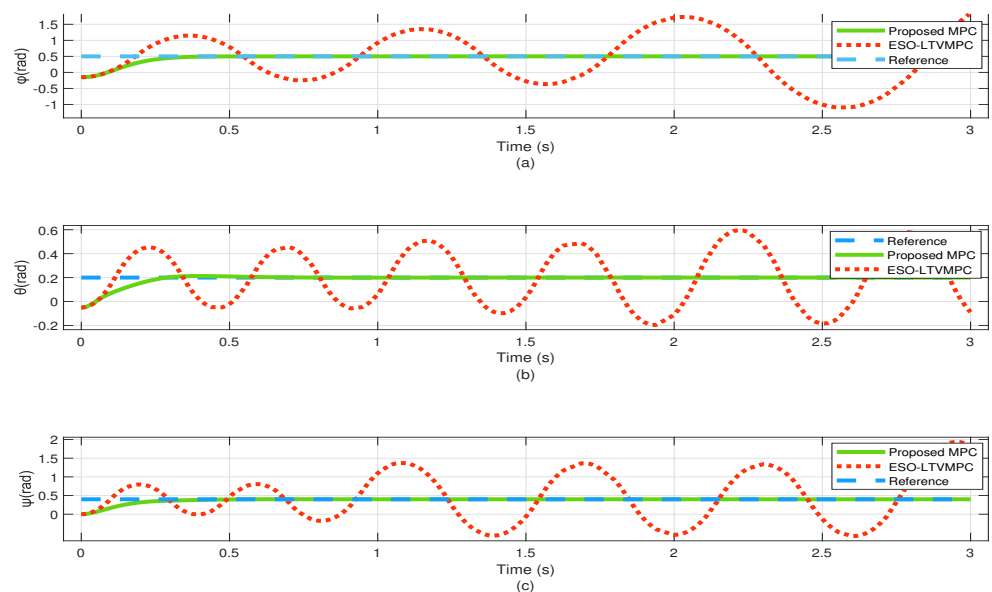


**Figure 6.** The attitude angle tracking curve of the UAV after changing different initial states: (a) roll; (b) pitch; (c) yaw.

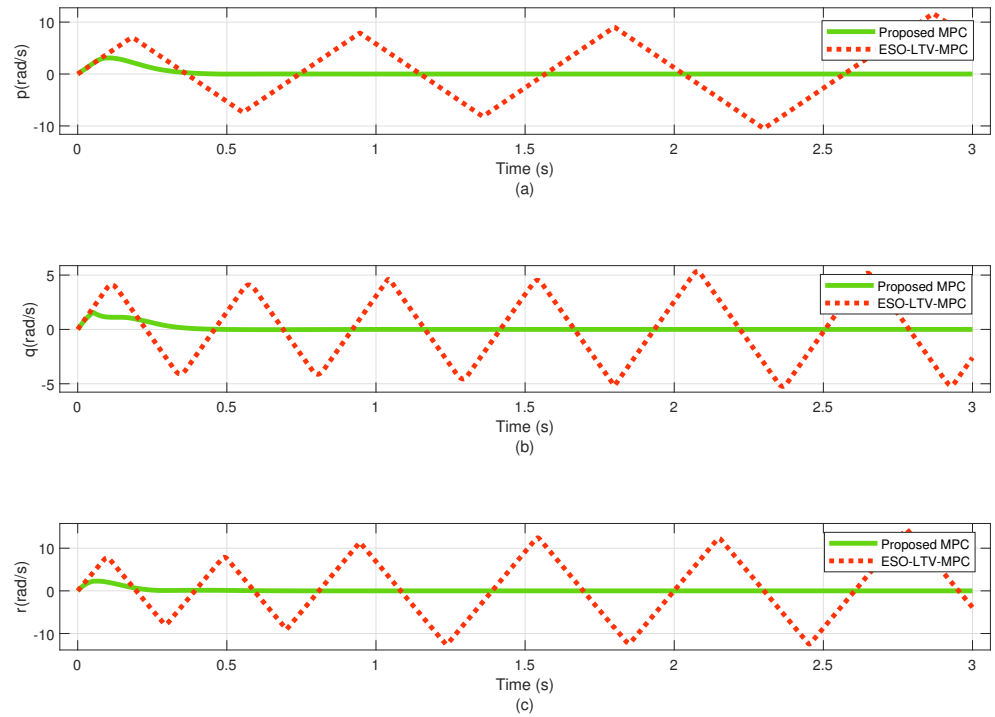


Figure 7. The velocity curve of the UAV after changing different initial states: (a)  $p$ ; (b)  $q$ ; (c)  $r$ .

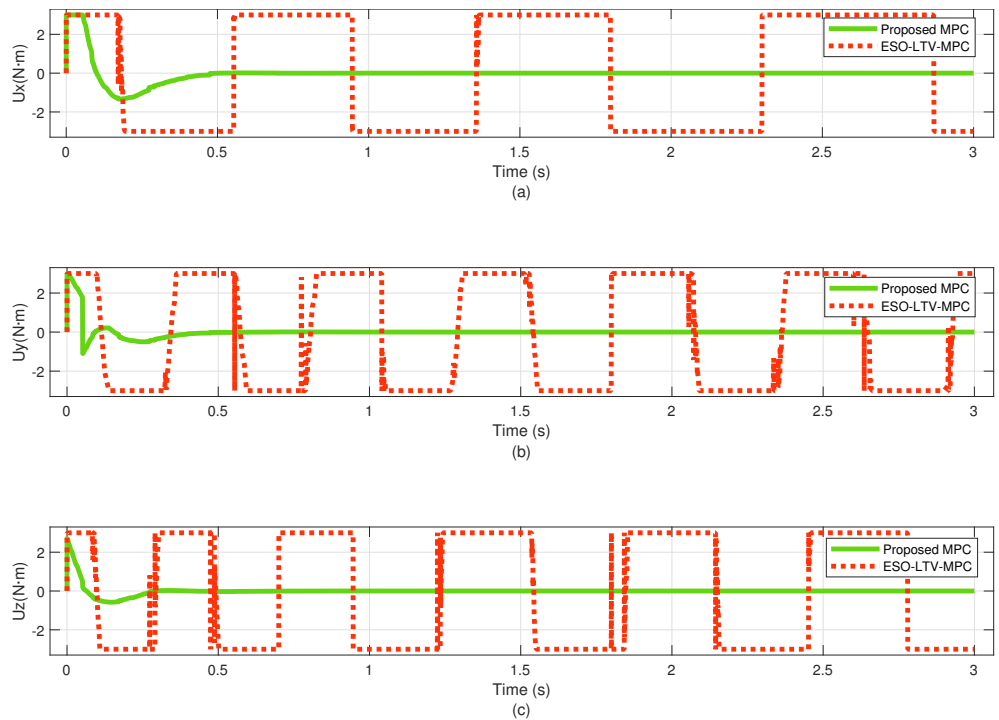


Figure 8. The input curve of the UAV after changing different initial states: (a)  $U_x$ ; (b)  $U_y$ ; (c)  $U_z$ .

#### 4.2. Flight Experiment

To evaluate the performance of the algorithm, we conducted flight experiments. The experiment used a self-developed flight controller. It uses STM32F765 (STMicroelectronics, Geneva, Switzerland) as the main control chip and is equipped with three-axis accelerometer and gyroscope MPU6000 (InvenSense, San Jose, CA, USA), accelerometer ICM-20602 (InvenSense, San Jose, CA, USA), and barometer MS5611 (MEAS Switzerland Sarl, Murten,

Switzerland). Through the extended Kalman filter algorithm, the real-time attitude and the heading angle are provided as state feedback information for the control system.

In the experiment, we tested the controller's performance by continuously changing the desired roll angle. To simulate continuous bounded disturbances, we used an electric fan to blow air in the direction of the drone's roll angle. The experimental results are shown as follows. As shown in the figure, the drone achieved hover at approximately 2 s and completed the experiment with a landing at around 12 s. The actual flight's roll angle control performance is depicted in Figure 9a. The rate of roll angle is demonstrated in Figure 9b. The PWM output values for the roll channel are shown in Figure 9c. When roll angle is 0, the PWM value should be in the middle value 1540. It is observed that the roll rate quickly changes in response to the variations in the reference roll angle under the controller's regulation. Therefore, as shown in Figure 9a, we can see that the drone exhibits good angle tracking performance.

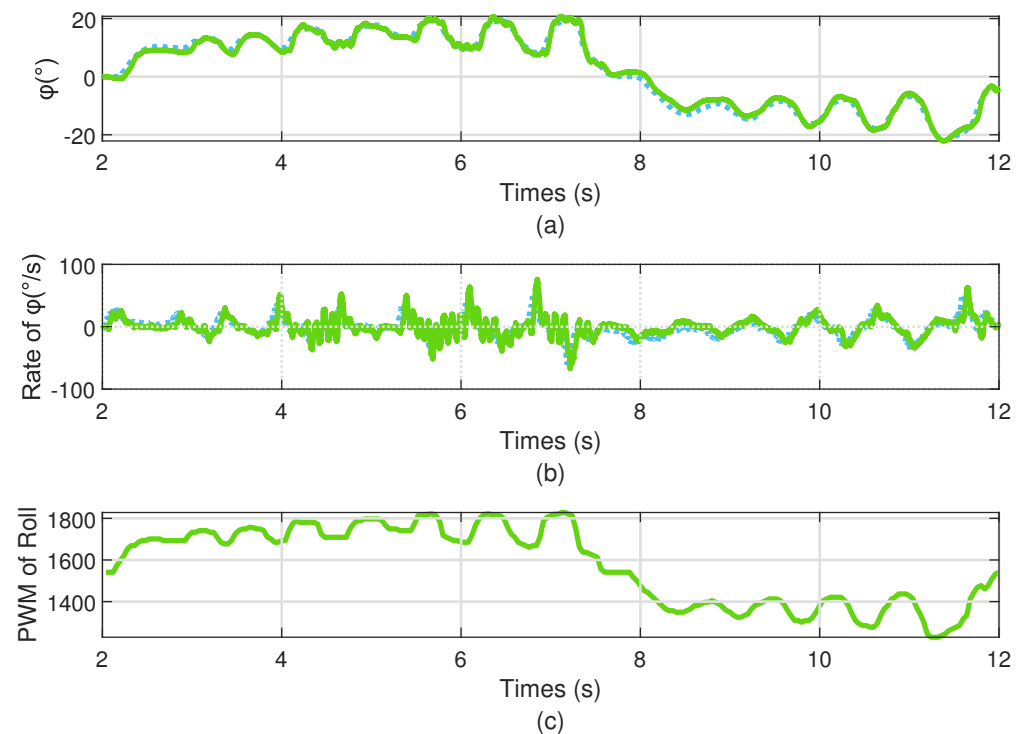


**Figure 9.** The actual state change of the drone roll angle channel: (a) the roll; (b) the rate for the roll channel; (c) the PWM output values for the roll channel. Green dotted lines are the actual angle, rate and pwm output. The blue dotted lines are the expectations.

Finally, the control method proposed in this paper proves the effectiveness of the coaxial UAV attitude system. The diagram clearly shows that the control strategy has better robustness than the traditional control method and can adapt to more complex external environments.

## 5. Conclusions

This paper constructs an attitude control system for a coaxial helicopter under disturbances. The proposed control system is designed based on the linearized nominal model of the coaxial helicopter. The new controller uses artificially set equilibrium points as tracking targets, with the system's equilibrium as decision variables in the cost function, ensuring recursive stability of the system under continuous disturbance. An extended state observer is designed to estimate the unmeasurable disturbances in the predictive model. Finally, simulation experiments and flight experiments verify that the proposed method can smoothly track the reference attitude under disturbances without deviation.

**Author Contributions:** Conceptualization, Z.C. and W.J.; methodology, X.L.; formal analysis, X.L.; investigation, X.L.; writing—original draft preparation, X.L.; writing—review and editing, Z.C.; supervision, Z.C.; funding acquisition, Z.C. and W.J. All authors have read and agreed to the published version of the manuscript.

**Funding:** This work was supported in part by the Natural Science Foundation of Qingdao (No. 23-2-1-122-zyyd-jch), National Natural Science Foundations of China under Grant No. 61903241 and No. 62303256, the China Postdoctoral Science Foundation under Grant 2018M630424, and Shandong Higher Education Youth Innovation and Science Fund Support Program (No. 2023KJ362).

**Data Availability Statement:** Data are contained within the article.

**Conflicts of Interest:** The authors declare no conflicts of interest.

## References

1. Maaruf, M.; Mahmoud, M.S.; Ma'arif, A. A survey of control methods for quadrotor UAV. *Int. J. Robot. Control Syst.* **2022**, *2*, 652–665. [[CrossRef](#)]
2. Pan, J.; Shao, B.; Xiong, J.; Zhang, Q. Attitude control of quadrotor UAVs based on adaptive sliding mode. *Int. J. Control Autom. Syst.* **2023**, *21*, 2698–2707. [[CrossRef](#)]
3. Liu, K.; Yang, P.; Wang, R.; Jiao, L.; Li, T.; Zhang, J. Observer-based adaptive fuzzy finite-time attitude control for quadrotor UAVs. *IEEE Trans. Aerosp. Electron Syst.* **2023**, *59*, 8637–8654. [[CrossRef](#)]
4. Lopez-Sanchez, I.; Pérez-Alcocer, R.; Moreno-Valenzuela, J. Trajectory tracking double two-loop adaptive neural network control for a Quadrotor. *J. Franklin Inst.* **2023**, *360*, 3770–3799. [[CrossRef](#)]
5. Liu, H.; Li, B.; Xiao, B.; Ran, D.; Zhang, C. Reinforcement learning-based tracking control for a quadrotor unmanned aerial vehicle under external disturbances. *Int. J. Robust Nonlinear Control* **2023**, *33*, 10360–10377. [[CrossRef](#)]
6. Miranda-Colorado, R.; Aguilar, L.T. Robust PID control of quadrotors with power reduction analysis. *ISA Trans.* **2020**, *98*, 47–62. [[CrossRef](#)]
7. Noormohammadi-Asl, A.; Esrafilian, O.; Arzati, M.A.; Taghirad, H.D. System identification and H-based control of quadrotor attitude. *Mech. Syst. Signal Process* **2020**, *135*, 106358. [[CrossRef](#)]
8. Hossam, A.; El-Badawy, A. Mu-based trajectory tracking control for a quad-rotor UAV. *Control. Theory Technol.* **2022**, *20*, 536–554. [[CrossRef](#)]
9. Jiang, W.; Ge, S.S.; Hu, Q.; Li, D. Sliding-Mode Control for Perturbed MIMO Systems With Time-Synchronized Convergence. *IEEE Trans. Cybern.* **2023**, *in press*. [[CrossRef](#)]
10. Jiang, W.; Ge, S.S.; Hu, Q.L. Fixed-time-synchronized control: A system-dimension-categorized approach. *Sci. China Inf. Sci* **2023**, *66*, 172–203. [[CrossRef](#)]
11. Li, Y.; Huang, Y.; Li, D.; Sun, Y.; Liu, H.; Jin, Y. Flight Tracking Control for Helicopter Attitude and Altitude Systems Using Output Feedback Method under Full State Constraints. *Aerospace* **2023**, *10*, 696. [[CrossRef](#)]
12. Zhang, S.; Zhang, H.; Ji, K. Incremental Nonlinear Dynamic Inversion Attitude Control for Helicopter with Actuator Delay and Saturation. *Aerospace* **2023**, *10*, 521. [[CrossRef](#)]
13. Wang, D.; Pan, Q.; Shi, Y.; Hu, J.; Zhao, C. Efficient Nonlinear Model Predictive Control for Quadrotor Trajectory Tracking: Algorithms and Experiment. *IEEE Trans Cybern* **2021**, *51*, 5057–5068. [[CrossRef](#)]
14. Liu, M.; Zhang, F.; Lang, S. The Quadrotor Position Control Based on MPC with Adaptation. In Proceedings of the 2021 40th Chinese Control Conference (CCC), Shanghai, China, 26–28 July 2021.
15. Dai, P.D.; Quoc, D.V.; Hai, D.M. Nonlinear Model Predictive Control for Quadrotors Using Simultaneous Optimization Approach. In Proceedings of the 2023 12th International Conference on Control, Automation and Information Sciences (ICCAIS), Hanoi, Vietnam, 27–29 November 2023.
16. Wang, P.; Dai, L.; Xue, R.; Huo, D.; Xia, Y. Ground Moving Target Tracking with Quadrotors using Nonlinear Model Predictive Control. In Proceedings of the 2022 China Automation Congress (CAC), Xiamen, China, 25–27 November 2022.
17. Filho, J.O.D.A.L.; Lourenço, T.S.; Fortaleza, E.; Murilo, A.; Lopes, R.V. Trajectory tracking for a quadrotor system: A flatness-based nonlinear predictive control approach. In Proceedings of the 2016 IEEE Conference on Control Applications (CCA), Buenos Aires, Argentina, 19–22 September 2016.
18. Bicego, D.; Mazzetto, J.; Carli, R.; Farina, M.; Franchi, A. Nonlinear Model Predictive Control with Enhanced Actuator Model for Multi-Rotor Aerial Vehicles with Generic Designs. *J. Intell. Robot. Syst.* **2020**, *100*, 1213–1247. [[CrossRef](#)]
19. Okulski, M.; Ławryńczuk, M. A Novel Neural Network Model Applied to Modeling of a Tandem-Wing Quadplane Drone. *IEEE Access* **2021**, *9*, 14159–14178.
20. Torrente, G.; Kaufmann, E.; Föhn, P.; Scaramuzza, D. Data-Driven MPC for Quadrotors. *IEEE Robot. Autom. Lett.* **2021**, *6*, 3769–3776. [[CrossRef](#)]
21. Romero, A.; Sun, S.; Foehn, P.; Scaramuzza, D. Model Predictive Contouring Control for Time-Optimal Quadrotor Flight. *IEEE Trans. Robot.* **2022**, *38*, 3340–3356. [[CrossRef](#)]

22. Salzmann, T.; Kaufmann, E.; Arrizabalaga, J.; Pavone, M.; Scaramuzza, D.; Ryll, M. Real-Time Neural MPC: Deep Learning Model Predictive Control for Quadrotors and Agile Robotic Platforms. *IEEE Robot. Autom. Lett.* **2023**, *8*, 2397–2404. [[CrossRef](#)]
23. Saviolo, A.; Li, G.; Loianno, G. Physics-Inspired Temporal Learning of Quadrotor Dynamics for Accurate Model Predictive Trajectory Tracking. *IEEE Robot. Autom. Lett.* **2022**, *7*, 10256–10263. [[CrossRef](#)]
24. Berberich, J.; Köhler, J.; Müller, M.A.; Allgöwer, F. Linear tracking MPC for nonlinear systems—Part I: The model-based case. *IEEE Trans. Automat. Contr.* **2022**, *67*, 4390–4405. [[CrossRef](#)]
25. Limon, D.; Ferramosca, A.; Alvarado, I.; Alamo, T. Nonlinear MPC for tracking piece-wise constant reference signals. *IEEE Trans. Automat. Contr.* **2018**, *63*, 3735–3750. [[CrossRef](#)]
26. Mayne, D.Q.; Rawlings, J.B.; Rao, C.V.; Scokaert, P.O.M. Constrained model predictive control: Stability and optimality. *Automatica* **2000**, *36*, 789–814. [[CrossRef](#)]
27. Berberich, J.; Köhler, J.; Müller, M.A.; Allgöwer, F. Linear tracking MPC for nonlinear systems—Part II: The data-driven case. *IEEE Trans. Automat. Contr.* **2022**, *67*, 4406–4421. [[CrossRef](#)]

**Disclaimer/Publisher’s Note:** The statements, opinions and data contained in all publications are solely those of the individual author(s) and contributor(s) and not of MDPI and/or the editor(s). MDPI and/or the editor(s) disclaim responsibility for any injury to people or property resulting from any ideas, methods, instructions or products referred to in the content.